

This is a postprint version of the following published document:

Puig-Rigall, J., Fernández-Rubio, C., González-Benito, J., Houston, J. E., Radulescu, A., Nguewa, P. & González-Gaitano, G. (2020). Structural characterization by scattering and spectroscopic methods and biological evaluation of polymeric micelles of poloxamines and TPGS as nanocarriers for miltefosine delivery. *International Journal of Pharmaceutics*, 578, 119057.

DOI: [10.1016/j.ijpharm.2020.119057](https://doi.org/10.1016/j.ijpharm.2020.119057)

© 2020 Elsevier B.V.



This work is licensed under a [Creative Commons Attribution-NonCommercial-NoDerivatives 4.0 International License](https://creativecommons.org/licenses/by-nc-nd/4.0/).

**Structural characterization by scattering and spectroscopic methods and biological  
evaluation of polymeric micelles of poloxamines and TPGS as nanocarriers for  
miltefosine delivery**

Joan Puig-Rigall<sup>a</sup>, Celia Fernandez-Rubio<sup>b</sup>, Javier González-Benito<sup>c</sup>, Judith Houston<sup>d</sup>,

Aurel Radulescu<sup>d</sup>, Paul Nguewa<sup>b,\*</sup>, Gustavo González-Gaitano<sup>a,\*</sup>

<sup>a</sup> Departamento de Química, Facultad de Ciencias, Universidad de Navarra, 31080

Pamplona, SPAIN

<sup>b</sup> University of Navarra, ISTUN Instituto de Salud Tropical, Department of

Microbiology and Parasitology. Irunlarrea 1, 31008 Pamplona, SPAIN

<sup>c</sup> Department of Materials Science and Engineering, IQMAAB, Universidad Carlos III

de Madrid, Av. Universidad 30, 28911 Leganés, SPAIN

<sup>d</sup> Jülich Center for Neutron Science, JCNS at Heinz Maier-Leibnitz Zentrum,

Forschungszentrum Jülich GmbH, Lichtenbergstraße 1, 85747 Garching, Germany

\*Corresponding authors: [gaitano@unav.es](mailto:gaitano@unav.es), [panguewa@unav.es](mailto:panguewa@unav.es)

## Abstract

for the treatment against leishmaniasis, a neglected tropical disease considered the world's second leading cause of death by a parasitic agent after malaria. MF exhibits dose-limiting gastrointestinal side effects in patients and its penetration through lipophilic barriers is reduced. In this work we propose a reformulation of MF by incorporating the drug to poly(ethylene)oxide (PEO)-based polymeric micelles, specifically, D- $\alpha$ -tocopheryl polyethylene glycol succinate (TPGS) and Tetronic block copolymers (T904 and T1107). A full structural characterization of the aggregates has been carried out by SANS (small-angle neutron scattering) and dynamic light scattering (DLS), in combination with proton 1D and 2D NMR spectroscopy, to determine the precise location of the drug. The structure of MF micelles has been characterized as a function of the temperature and concentration. In the presence of the polymers, MF forms mixed micelles in a wide range of temperatures, TPGS being the co-surfactant that incorporates more MF unimers. The hydrophobic parts of MF and the block copolymers are in close contact within the micelles, which present a core-shell structure with a hydrophilic corona formed by the PEG blocks of the TPGS and the zwitterion head of the MF. With the aim of exploring gel-based formulations of the drug, the combination of MF and T1107 under gelation conditions has also been investigated. In order to identify the best carrier, the antileishmanicidal activity of MF in the different formulations has been tested on macrophages, promastigotes and intracellular amastigotes. The combination of the three vehicles with MF makes the formulated drug more active than MF alone against *L. major* promastigotes, however, only the combination with T904 increases the MF activity against intracellular amastigotes.

**Keywords:** miltefosine, Tetronic, poloxamine, TPGS, micelles, gels, cytotoxicity,  
SANS

## 1. INTRODUCTION

Leishmaniasis is a group of diseases caused by parasites of the *Leishmania* genus transmitted by female sand flies. Different clinical forms of the leishmaniasis are known, being the cutaneous leishmaniasis (CL) the most common form of the disease, which manifests in skin ulcers generally resulting in disfiguring scars and lesions.<sup>1,2</sup> Currently, no effective human vaccines are available and antileishmaniasis drugs are unaffordable for most of the affected people. A large number of antitumoral compounds have demonstrated activity to treat the disease,<sup>3,4</sup> although the only oral drug reported to have an effect against *Leishmania* parasite is miltefosine (MF), an alkylphospholipid originally developed for breast cancer treatment.<sup>5,6</sup>

When compared to the current first-line therapies, MF is more cost-effective,<sup>7</sup> and several studies have suggested its application against leishmaniasis using different formulations.<sup>8-15</sup> However, it exhibits dose-limiting gastrointestinal side effects in patients<sup>16</sup> because MF penetration through lipophilic barriers is reduced due to its poor aqueous solubility with the formation highly hemolytic micelles at low concentration, which easily disaggregate under oral or intravenous administration.<sup>17</sup> Therefore, the use of drug carriers may be helpful to improve drug penetration into the skin and control drug release.

The first nanocarriers designed to control the MF release were liposomes. However, their used in drug delivery was limited for its poor stability.<sup>18</sup> An alternative to prevent MF side effects are polymeric micelles, which are interesting due to their appropriate size. Some studies have described MF-loaded polymeric micelles of poloxamers or Pluronic,<sup>19,20</sup> triblock copolymers of poly(ethylene oxide)-poly(propylene oxide)-poly(ethylene oxide) (PEO-PPO-PEO) that differs in the relative length of PEO and PPO blocks, giving different micellization and gel-transition behaviour depending on

the temperature.<sup>21-23</sup> However, some other copolymers with different properties and behaviours can be used.

One of the possibilities is the first copolymer studied in this work D- $\alpha$ -tocopheryl polyethylene glycol succinate, TPGS, a water soluble derivative of the natural form of vitamin E, where the D- $\alpha$ -tocopheryl succinate is esterified with a short polyethylene glycol (PEG) chain.<sup>24</sup> It has been approved by the Food and Drug Administration (FDA) and investigated for its capacity to solubilize hydrophobic substances in drug delivery.<sup>25,26</sup> CMC value of 0.02% is obtained for TPGS, where micelles present a core-shell architecture with high aggregation number ( $N_{agg} \approx 100$ ) and highly hydrated PEO corona, characterized for its stability with temperature and concentration, which is an important advantage for their use in pharmaceutical field.<sup>27</sup>

On the other hand, Poloxamines, also known by their commercial name of Tetronics (BASF), are the other type of copolymer studied as potential carriers of MF. They share with Pluronics the PEO and PPO blocks, as well as the amphiphilic character and self-assembly behaviour as a function of temperature and concentration. They are octablock copolymers of PEO and PPO, distributed into four arms connected by a central ethylene diamine spacer, which can be protonated/deprotonated according to the pH of the environment, providing the pH-responsiveness in the micellization and gelation processes of poloxamines.<sup>28-31</sup>

Within this framework, we have investigated the structures formed when TPGS and Tetronics 904 (T904) and 1107 (T1107) interact with MF, in view of potential applications where polymeric micelles are used as vehicle for MF. The Tetronics were selected considering their length and HLB, being T904 relatively short and lipophilic, while the larger T1107 can form gels under certain conditions. The micellization of the MF was first studied by dynamic light scattering (DLS) and small-angle neutron

scattering (SANS). These techniques were also used when the MF is mixed with the copolymers under diluted conditions, as well as 1D and 2D NMR to determine the precise location of the drug in the micelles. Also, the behavior of MF and T1107 under the gelation of the system was investigated by SANS experiments. Finally, biological studies in promastigotes and amastigotes were performed to study the activity of MF in the different formulations.

## **2. MATERIALS AND METHODS**

**2.1 Materials.** Tetronic 904 (T904) and 1107 (T1107) were a gift from BASF. The composition per arm of T904 is 15 EO and 17 PO, with average molecular weight of 6,700 g mol<sup>-1</sup>. The composition per arm of T1107 is 60 EO and 20 PO (average molecular weight of 15,000 g mol<sup>-1</sup>). D- $\alpha$ -tocopheryl polyethylene glycol succinate (TPGS) was a gift from Antares Health Products Inc, with a molecular weight of the polyethylene glycol part, PEG, of 1000 g mol<sup>-1</sup> (23 EO units). All the solutions were prepared weighting out, and the concentrations were expressed in wt%, unless stated otherwise. Our reference drug Miltefosine (MF) was purchased from Sigma-Aldrich (St. Louis, MO, USA).

**2.2 Small-angle neutron scattering (SANS).** SANS experiments were carried out on the KWS-2 diffractometer at the Jülich Centre for Neutron Science (JCNS), Munich, Germany.<sup>32</sup> An incidental wavelength of 5 Å was used with detector distances of 1.7 and 7.6 m, with a collimation length of 8 m, to cover the q range from 0.008 to 0.5 Å<sup>-1</sup>. In the standard mode a wavelength spread  $\Delta\lambda/\lambda=20\%$  was used, while in the concentrated regime, a high-resolution mode was achieved by using a collimation length of 20 m in combination with the double-disc chopper and time-of-flight data acquisition for an improved wavelength spread of  $\Delta\lambda/\lambda=5\%$ . All samples were

measured in rectangular quartz cells (Hellma) with a path length of 2 mm using D<sub>2</sub>O as the solvent (Aldrich, 99.9% in D). The samples were placed in an aluminium rack where water was recirculated from an external Julabo cryostat, ranging temperatures from 20 °C to 50 °C. This set-up enables a thermal control with up to 0.1 °C precision. Scattered intensities were corrected for detector pixel efficiency, empty cell scattering and background due to electronic noise. The data were set to absolute scale using Plexiglas as a secondary standard. The obtained macroscopic differential cross-section  $d\Sigma/d\Omega$  was further corrected for the contribution from the solvent. The complete data reduction process was performed with the QtiKWS software provided by JCNS in Garching. Data analysis was carried out with Sasview 4.2.0 software (<http://www.sasview.org/>) considering the instrumental smearing. Levenberg-Marquardt algorithm was chosen in each case prior to an in-depth study using the implemented optimizer DREAM, in order to better estimate the uncertainties of the fitted parameters. The scattering curves from the micelles were fitted to a core-shell sphere (CSS) model combined with a hard-sphere (HS) structure factor, while the analysis of the gels scattering was carried out using a body-centred cubic paracrystalline model (BCC). More details on the models used are provided in Supporting Information.

**2.3 Dynamic light scattering (DLS).** DLS measurements were carried out using a DynaPro-MS/X photon correlation spectrometer with a laser wavelength of 822 nm at a fixed scattering angle of 90°. The temperature was controlled in the cell with the built-in Peltier unit, with 0.1 °C accuracy. The intensity size distributions were obtained from the autocorrelation function, considering the viscosities and refractive indexes of the solvent at each temperature (D<sub>2</sub>O, to reproduce SANS conditions) with the implemented software Dynamics V6. Samples were filtered through 0.22 µm PVDF syringe filters

prior to the measurements. The samples for the experiments with MF alone were filtered through 0.02  $\mu\text{m}$  filters.

**2.4 Nuclear Magnetic Resonance Spectroscopy (NMR).** Both monodimensional and 2D-NOESY proton spectra were recorded on a Bruker Avance Neo 400 spectrometer. The temperature in the probe was controlled according to the sample type. The samples were prepared in  $\text{D}_2\text{O}$  (Aldrich >99.9% in deuterium).

## **2.5 Biological evaluations**

### **2.5.1 Cells and culture conditions**

*Leishmania major* promastigotes (Lv39c5) were grown at 26°C in M199 medium supplemented with 25 mM HEPES (pH 7.2), 0.1 mM adenine, 0.0005% (wt/vol) hemin, 2 mg/ml biopterin, 0.0001% (wt/vol) biotin, 10% (vol/vol) heat-inactivated fetal bovine serum (FBS), and an antibiotic cocktail (50 U/ml penicillin, 50 mg/ml streptomycin). To maintain their infectivity, *Leishmania* cells were isolated from infected BALB/c mouse spleen and parasites were maintained in culture for not more than five passages. Murine peritoneal macrophages from 4- to 6-week-old BALB/c mice were used for the study. Animals were inoculated with 2 ml sterile thioglycolate (3%) broth (BD Difco) prior to peritoneal cavity lavage with 5 ml of cold RPMI medium, and macrophages were removed by a syringe. All the procedures involving animals were approved by the Animal Care Ethics Commission of the University of Navarra.

### **2.5.2 Leishmanicidal activity**

#### **2.5.2.1 Activity against promastigotes**

To determine the antileishmanial activities of the compounds analyzed in this study, exponentially growing cells ( $2 \times 10^6$  *L. major* promastigotes/ml) were seeded in 96-well plates (100  $\mu\text{l}$  per well) with increasing concentrations of the compounds. Stock

aqueous solutions of 0.2% (5mM) MF, 1% Polymer and 1% Polymer + 0.2% MF were diluted in 100 µl of M199 medium (obtaining the corresponding concentrations) and maintained at 26°C. After 72 h of incubation, the half-maximal effective concentration (EC<sub>50</sub>) was calculated by the MTT test (Sigma, St. Louis, MO, USA), which was also performed to determine the cytotoxicity of selected compounds in Bone-marrow-derived macrophage (BMDM). MTT solutions were prepared at 5 mg/ml in phosphate-buffered saline (PBS), filtered and maintained at -20°C until use. After 72 h of incubation, 100 µg/well of MTT were added and the plates were incubated 4 h under the same conditions. Therefore, 80 µl of a dimethyl sulfoxide were added to each well to dissolve formazan crystals. The optical density (OD) was measured in a Multiskan EX microplate photometer plate reader at 540 nm and EC<sub>50</sub> was calculated. The EC<sub>50</sub> represents the concentration required for to effect against the viability of 50% of promastigotes of treated cells with respect to untreated cells (controls). This parameter was obtained by fitting a sigmoidal Emax model to dose-response curves. The results were expressed as means (± standard deviation, SD) from two independent experiments.

#### **2.5.2.2 Activity against intracellular amastigotes**

Murine peritoneal macrophages were seeded in 8-well culture chamber slides (Lab-Tek™; BD Biosciences) at a density of  $5 \times 10^4$  cells per well in Roswell Park Memorial Institute (RPMI) medium and allowed to adhere overnight at 37°C in a 5% CO<sub>2</sub> incubator. In order to perform the infection assay, metacyclic *L. major* promastigotes isolated by the peanut agglutinin (PNA) method were used to infect macrophages at a macrophage/parasite ratio of 1/20. The plates were incubated for 24 h under the same conditions until promastigotes were phagocytized by macrophages. The wells were then washed with medium to remove the extracellular promastigotes, and plates were incubated with fresh medium supplemented with increasing concentrations of drug.

Dilutions of stock aqueous solutions of 0.2% (5mM) MF, 1% Polymer and 1% Polymer + 0.2% MF were done. Forty-eight hours later, cells were washed with PBS, fixed with ice-cold methanol for 5 min, and stained with Giemsa stain. To determine parasite burden, the number of infected macrophages per at least 200 macrophages was counted under a light microscope. The percentage of infected macrophage was determined by dividing the total number of infected macrophages counted by the corresponding number of macrophages. Three independent experiments were performed with duplicates.

### **2.5.3 Statistical analysis**

Statistical analyses were performed using PRISM version 5.0 (GraphPad). Data are presented as mean  $\pm$  SD. Comparisons between two groups were made using Mann Whitney or two-tailed unpaired t-test. Statistical significance was assigned to  $p < 0.001$  (\*\*\*),  $p < 0.01$  (\*\*) or  $p < 0.05$  (\*).

## **3. RESULTS AND DISCUSSION**

### *3.1 Characterization of miltefosine micelles*

MF is a zwitterionic amphiphile which self-aggregates in water forming micelles. Values of critical micellar concentration (*cmc*) of MF in aqueous solutions range from 2.0 to 160  $\mu$ M, depending of the technique used.<sup>33,34</sup> By using DLS, at 0.2% MF, well above the CMCs, reported micelles of  $R_h = 3.5$  nm can be observed at 20 and 37  $^{\circ}$ C, in accordance with literature values,<sup>19</sup> while slightly smaller sizes are obtained at 50  $^{\circ}$ C ( $R_h = 3.0$  nm). At higher concentration of the surfactant (1%), no temperature effect can be appreciated on MF micelles, with hydrodynamic radius of 3.0 nm (SI, Figure 1).

More detailed information on the micelles structure can be obtained by SANS. The scattering patterns as a function of temperature are plotted in Figure 1. The curves have been fitted to a CSS-HS model, in which the scattering length density ( $sld$ ) values of the core (aliphatic chain) has been fixed at  $-3.73 \cdot 10^{-7} \text{ \AA}^{-2}$  (see SI for details on the calculations). The aggregation number of the micelles and the fraction of water in the shell were obtained following the calculations described elsewhere,<sup>27</sup> considering a value of  $sld = 1.30 \cdot 10^{-6} \text{ \AA}^{-2}$  for hydrophilic head of MF in accordance with literature.<sup>35</sup> Polydispersity was fixed at 0.15 considering the DLS results. All the relevant structural data obtained are gathered in Table 1.

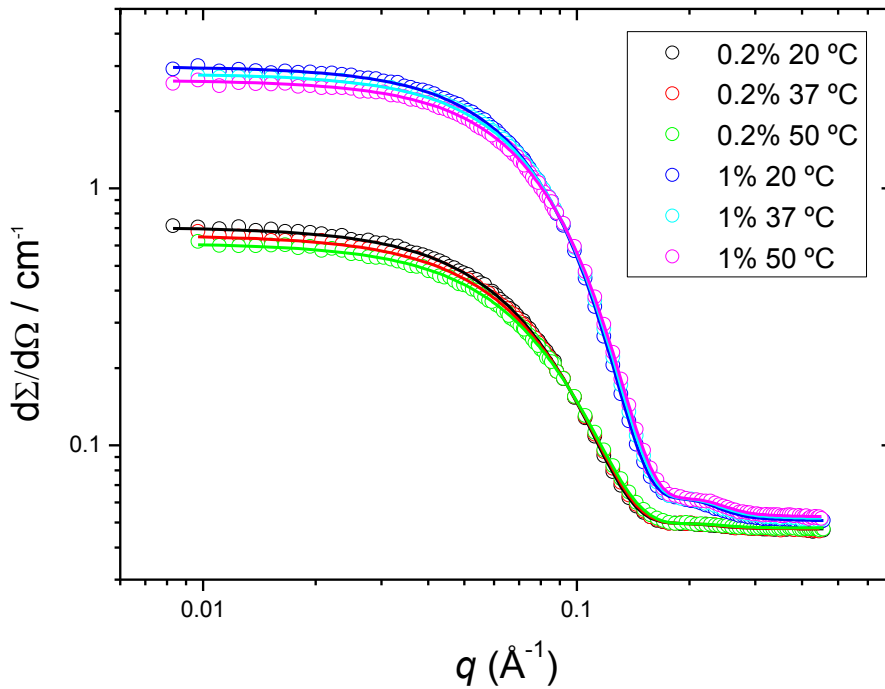


**Figure 1.** SANS curves of 0.2% and 1% MF in D<sub>2</sub>O at 20, 37 and 50 °C. Solid lines correspond to the fits to a CSS-HS model

**Table 1.** Structural parameters of MF micelles in D<sub>2</sub>O as a function of the temperature deduced from SANS data analysis.  $R_c$  (core radius, Å),  $t$  (shell thickness, Å),  $\phi$  (volume fraction),  $\rho_s$  (shell scattering length density  $\times 10^6 \text{ \AA}^{-2}$ ),  $X_{D_2Oshell}$  (fraction of water in the shell),  $N_{agg}$  (aggregation number of micelles)

| % MF | $T / ^\circ\text{C}$ | $R_c$ | $t$ | $\phi$ | $\rho_s$ | $X_{D_2Oshell}$ | $N_{agg}$ |
|------|----------------------|-------|-----|--------|----------|-----------------|-----------|
| 0.2  | 20                   | 24    | 7   | 0.003  | 5.24     | 0.779           | 106       |
|      | 37                   | 24    | 6   | 0.003  | 5.10     | 0.751           | 99        |
|      | 50                   | 23    | 7   | 0.003  | 5.02     | 0.735           | 93        |
| 1.0  | 20                   | 24    | 8   | 0.015  | 5.39     | 0.808           | 105       |
|      | 37                   | 24    | 8   | 0.016  | 5.48     | 0.826           | 98        |
|      | 50                   | 23    | 7   | 0.014  | 5.16     | 0.763           | 92        |

The fitted data reveal a total micelle size ( $R_c + t$ ) of 3–3.5 nm, as observed in DLS (SI, Figure 1). The micelles are stable with the temperature, slight reductions in their hydration of the shell and aggregation number,  $N_{agg}$ , are only observed as temperature increases (Table 1). Besides, no remarkable effects are observed in size and  $N_{agg}$  of MF micelles with concentration. But, volume fraction of micelles significantly increases, while a slightly high hydration of the shell is shown from 0.2% to 1%.

### 3.2 Structure of miltefosine loaded polymeric micelles

#### 3.2.1 Mixed TPGS-MF micelles

The first polymeric surfactant considered as a micellar vehicle for MF is TPGS, which has a *cmc* value of 0.02% and forms stable core-shell micelles in a wide range of temperatures and concentrations. By DLS, the size of 0.2% MF loaded 1% TPGS micelles in D<sub>2</sub>O is 10-11 nm, not different from the value of 10 nm reported for TPGS in water,<sup>27</sup> with a slight decrease with the temperature (Figure 2). SANS patterns of the mixed system are compared to unloaded 1% TPGS in SI, Figure 2. The curves are quite similar, they only differ in a slight reduction in the scattered intensity in the presence of

MF and a shift of the curves at any of the temperatures towards high  $q$ , indicating the reduction in size of the aggregates. The curves have been fitted to a CSS-HS model, but in this case the polydispersity has been left free, obtaining values close to 0.15. Table 2 shows all the relevant structural data obtained.

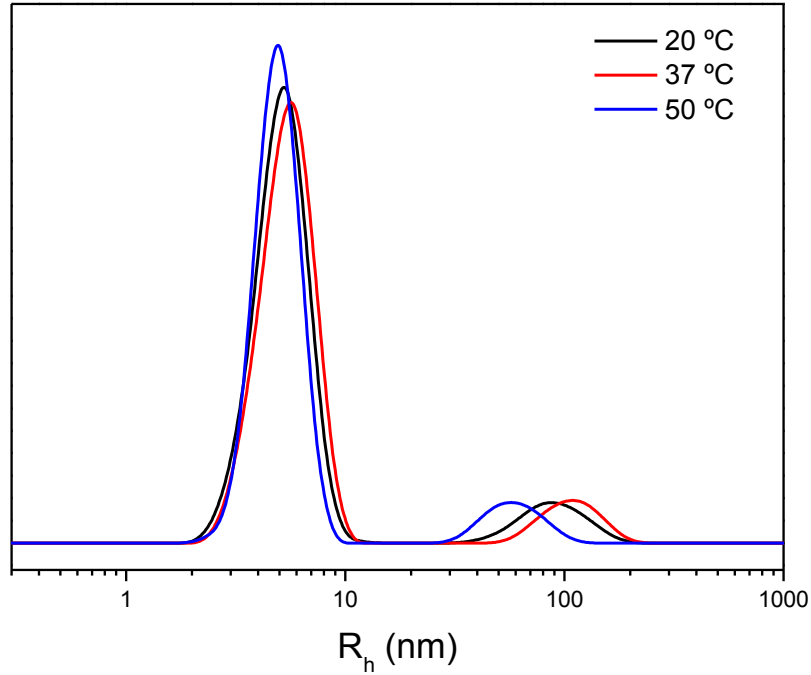


**Figure 2.** Size distributions obtained by DLS of 1% TPGS + 0.2% MF in D<sub>2</sub>O

**Table 2.** Structural parameters of TPGS and TPGS-MF mixed micelles in D<sub>2</sub>O as a function of the temperature deduced from SANS data analysis.  $R_c$  (core radius, Å),  $t$  (shell thickness, Å),  $\phi$  (volume fraction),  $\rho_s$  (shell scattering length density  $\times 10^6 \text{ \AA}^{-2}$ ),  $\rho_c$  (core scattering length density  $\times 10^6 \text{ \AA}^{-2}$ )

|                   | $T / ^\circ\text{C}$ | $R_c$ | $t$ | $\phi$ | $\rho_s$ | $\rho_c$ |
|-------------------|----------------------|-------|-----|--------|----------|----------|
| 1% TPGS           | 20                   | 32    | 30  | 0.028  | 5.55     | 0.28     |
|                   | 37                   | 34    | 29  | 0.027  | 5.65     | 0.28     |
|                   | 50                   | 35    | 28  | 0.026  | 5.70     | 0.28     |
| 1% TPGS + MF 0.2% | 20                   | 31    | 26  | 0.035  | 5.79     | 0.16     |
|                   | 37                   | 31    | 24  | 0.031  | 5.80     | 0.03     |

|  |    |    |    |       |      |       |
|--|----|----|----|-------|------|-------|
|  | 50 | 31 | 23 | 0.028 | 5.80 | -0.07 |
|--|----|----|----|-------|------|-------|

The fitted data for TPGS alone were done considering a "dry" core (the theoretical  $sld$  value assuming it is formed by a tocopherol moiety is  $2.8 \times 10^{-7} \text{ \AA}^{-2}$ ). The results reveal a highly hydrated shell and very stable micelles with temperature, in accordance with previous studies.<sup>27</sup> The presence of the MF produces a shrinking of the mixed micelle (reduction of ca. 11% in total size), and similar  $sld_{shell}$  values. However, somewhat lower  $sld_{core}$  are obtained as temperature increases, explainable in terms of the solubilisation of the hydrophobic part of the MF in the micellar core (considering that for MF  $sld_{core} = -3.73 \times 10^{-7} \text{ \AA}^{-2}$ ).

NMR spectroscopy has proven useful in determining the precise location of drugs dissolved in micelles.<sup>36</sup> Figure 3 shows the aliphatic region of the 1D proton spectrum obtained from a 1% TPGS + 0.2% MF mixture at 25°C, comparing with the substances alone. In the particular case of TPGS and MF combination, both surfactants share aliphatic moieties which are quite similar in terms of the NMR signals they produce. Yet, changes on representative protons of both surfactants are observed, which clearly indicate a change in the magnetic environment upon mixing.

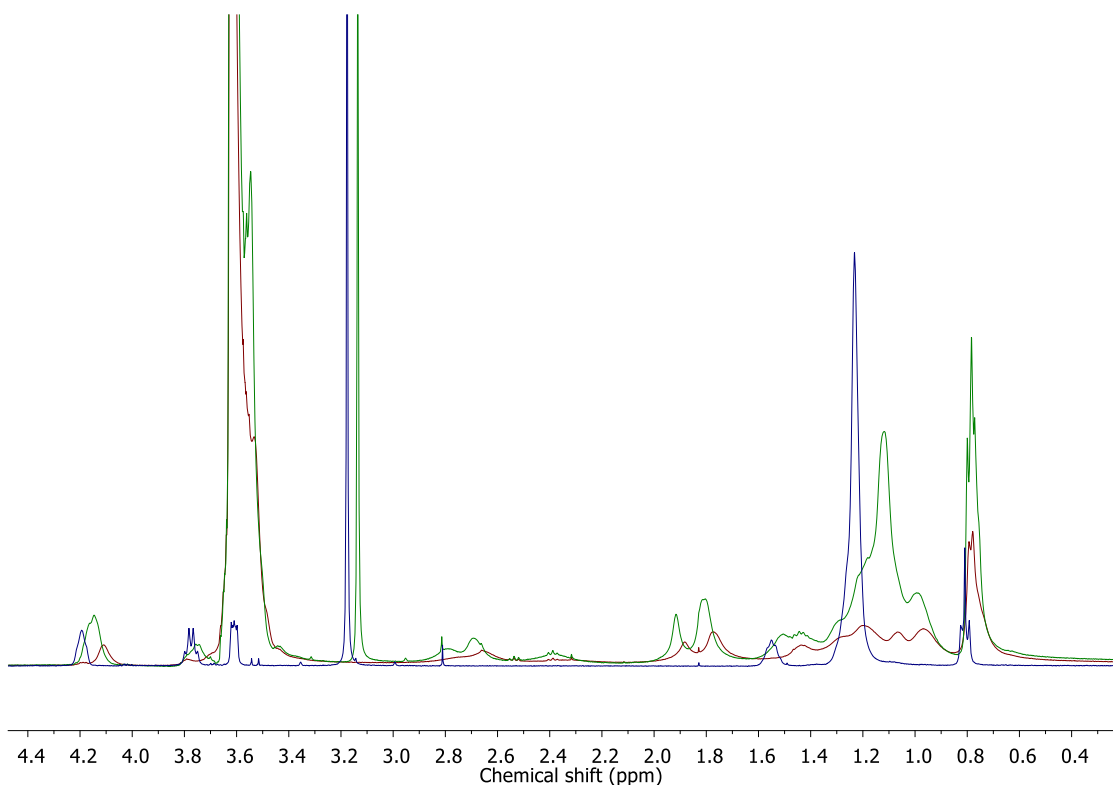


**Figure 3.**  $^1\text{H-NMR}$  spectra in  $\text{D}_2\text{O}$  of 0.2% MF (blue), 1% TPGS (red) and 1% TPGS + 0.2% MF (green) at 25 °C.

The most important changes occur in the methylene protons of the hydrophobic tail of MF (1.23 ppm, see SI-Figure 3 for signal assignment), which shift upfield (1.12 ppm), as well as the  $\text{CH}_3$  of the surfactant head, in a lesser extent (from 3.18 to 3.14 ppm). Changes are also detected in the TPGS protons of the hydrophobic part. Thus, in aliphatic zone between 1.0 and 1.5 ppm, which corresponds to the resonances of  $\text{CH}_3$ (a) and  $\text{CH}_2$ (b) of the tocopherol moiety of TPGS,<sup>27</sup> protons d and e (directly bonded to the aromatic ring, 1.92 and 1.81 ppm) increase their chemical shifts by 0.03 ppm with MF addition. By contrast, the PEG tail of TPGS (intense resonances of the EO residues at 3.64 ppm) remains unaltered. The 2D-NOESY spectrum, shown in Figure 4, help define the precise location of both surfactants in the micelles. The lack of any cross-peak between the characteristic bulky  $\text{CH}_3$  protons of the zwitterion head (3.2 ppm) and any of the tocopherol moiety of TPGS (0.8 – 2.5 ppm) indicates that the MF head must be located far from the core. In addition, there is a neat cross-peak between the methyl

group of MF with the bulky aromatic methyls, d and e of TPGS. The interactions between these protons and the hydrophobic chain of TPGS are also less intense than those observed in TPGS micelles (SI, Figure 4), which confirms the closeness between the hydrophobic parts of both surfactants. Overall, NMR evidence that MF and TPGS are forming a mixed micelle, in which the hydrophobic parts of both surfactants are in close contact, with a hydrophilic shell mainly formed by the PEG blocks of the TPGS and the zwitterion head of the MF.

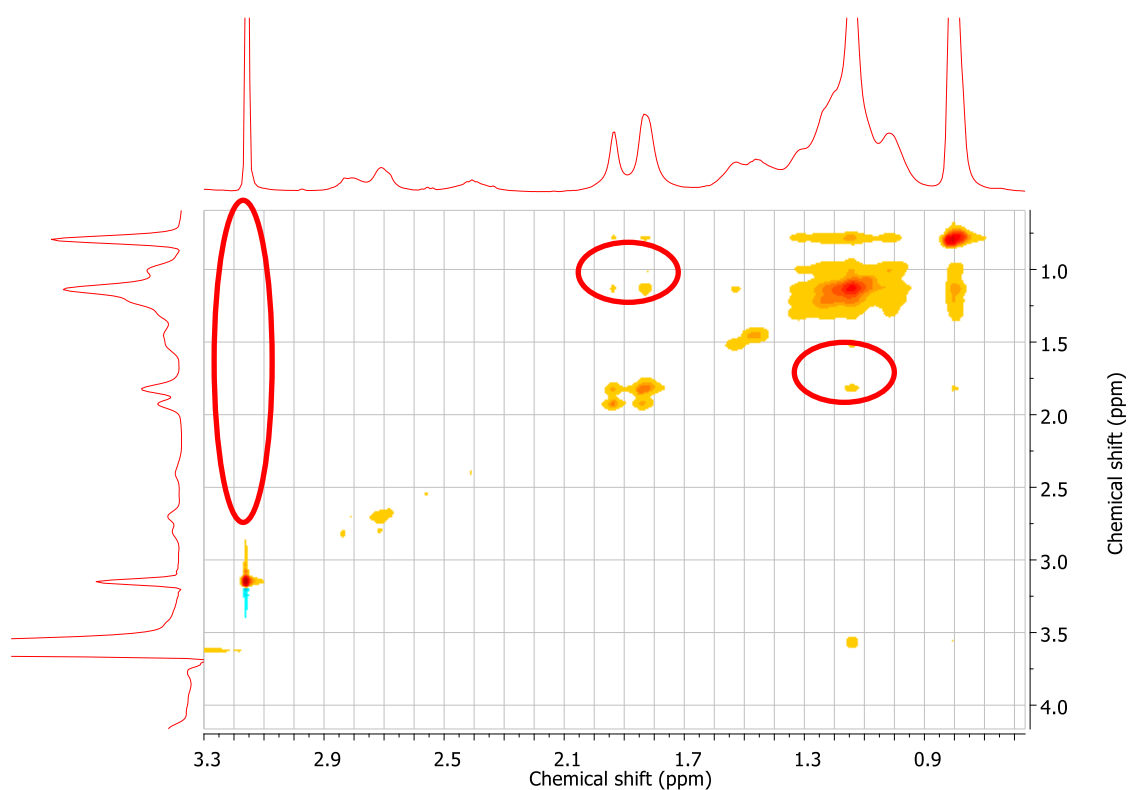


**Figure 4.** 2D-NOESY spectrum of 1% TPGS + 0.2% MF at 25 °C in D<sub>2</sub>O

It is possible to estimate the content of MF and TPGS in the mixed micelle from the SANS data by making some reasonable assumptions. Following NMR evidence, the MF must be located preferentially in the core, given its hydrophobic character, while the shell is formed mostly by the PEG chains. Assuming that the water content of the

micelle comes mainly from the hydration of the EO (the presence of solvent in the micelle core should be negligible), the volume of the core ( $V_c$ ) can be expressed as

$$V_c = v_{TPGS,c}N_{TPGS} + v_{MF,c}N_{MF} \quad (1)$$

where  $v_{TPGS,c}$  is the volume of the hydrophobic part of one TPGS molecule in the micelle,  $v_{MF,c}$  that of one MF molecule, and  $N_{TPGS}$  and  $N_{MF}$  the number of molecules of both surfactants per micelle. Likewise, the total volume of the micelle ( $V_m$ ) is defined as

$$V_m = (v_{TPGS} + n_{EO}n_{solv/EO}v_{D_2O})N_{TPGS} + v_{MF}N_{MF} \quad (2)$$

where  $v_{TPGS}$  and  $v_{MF}$  stand for the volume of TPGS and MF molecules, respectively,  $v_{D_2O}$  is the volume of a solvent molecule,  $n_{EO}$  the number of EO monomers that form the hydrophilic block (23 per TPGS molecule) and  $n_{solv/EO}$  the number of solvent molecules per EO monomer. These numbers can be calculated at each temperature if we consider the “pure” TPGS micelles, by means of

$$n_{solv} = \frac{\rho_{shell} - \rho_{EO}}{\rho_{D_2O} - \rho_{EO}} \frac{v_{shell}}{v_{D_2O}} \quad (3)$$

where  $n_{solv}$  and  $v_{shell}$  refer to the number of D<sub>2</sub>O molecules in the shell and the volume of the corona of the TPGS micelles, and  $\rho_{shell}$ ,  $\rho_{EO}$ ,  $\rho_{D_2O}$  correspond to the sld values deduced by SANS (Table 2), the EO ( $6.38 \times 10^{-6} \text{ \AA}^{-2}$ ) and solvent ( $6.36 \times 10^{-6} \text{ \AA}^{-2}$ ). The calculation yields values of  $n_{EO} = 10, 9.8$  and  $8.8$  at  $20, 37$  and  $50^\circ\text{C}$ , respectively, in agreement with our previous studies.<sup>27</sup>

The number of monomers of TPGS and MF in the micelles can be deduced by solving the system of equations (1) and (2), as well as their volume fractions in the mixed micelles. The results of these calculations are shown in Table 3, where it can be seen how the volume fraction of TPGS in the mixed micelles is always lower than half of the total volume. Interestingly, the combination with TPGS increases the aggregation

number observed in MF micelles (Table 1), with an increase in MF fraction with the temperature, while the number of TPGS unimers in the micelles is reduced.

**Table 3.** Number of molecules of MF ( $N_{MF}$ ) and co-surfactant (TPGS or Tetronics,  $N_{CS}$ ), volume and mass fraction of MF ( $\phi_{MF}$  and  $w_{MF}$ ) as deduced from SANS data analysis in mixed systems (the aggregation number of the pure co-surfactant micelles are between parentheses).

|                   | $T / ^\circ C$ | $N_{CS}$ | $N_{MF}$ | $\phi_{MF}$ | $w_{MF}$ |
|-------------------|----------------|----------|----------|-------------|----------|
| 1% TPGS + 0.2%MF  | 20             | 80 (118) | 139      | 0.36        | 0.32     |
|                   | 37             | 69 (125) | 161      | 0.43        | 0.39     |
|                   | 50             | 65 (125) | 172      | 0.47        | 0.42     |
| 1% T904 + 0.2%MF  | 37             | 12 (24)  | 74       | 0.30        | 0.27     |
|                   | 50             | 20 (31)  | 77       | 0.21        | 0.19     |
| 1% T1107 + 0.2%MF | 37             | 8 (11)   | 56       | 0.17        | 0.15     |
|                   | 50             | 14 (18)  | 78       | 0.15        | 0.13     |

### 3.2.2 Mixed Tetronic-MF micelles

As mentioned above, and as a difference to TPGS, Tetronic polymeric micelles are an interesting vehicle due to their capacity of producing a pH-triggered delivery, conferred by the middle diamine group. At moderate low concentrations and above 35°C both, T904 and T1107, form spherical micelles, with the core formed by the PPO blocks and the shell by the highly hydrated PEO blocks.<sup>28,30</sup> The size of the mixed micelles with MF has been determined by DLS as a function of temperature. Considering first the T904, a distribution with hydrodynamic radius of 3.5 nm is observed at 20 °C (SI, Figure 5), similar size to that of MF micelles ( $R_h = 3.3$  nm, SI, Figure 1), while no presence of T904 unimers is detected. At 37 °C and 50 °C, aggregates with a hydrodynamic radius of 5.2 nm are obtained (SI, Figure 5), slightly smaller than in

T904 “pure” micelles under the same conditions ( $R_h = 6$  nm).<sup>28</sup> When T1107 is used, bigger sizes than those of T1107 unimers ( $R_h = 3.3$  nm) and MF micelles are obtained, with  $R_h = 5.2$  nm (SI, Figure 6) at 20 °C, suggesting the incorporation of the non-aggregated T1107 to the MF micelles. As the temperature increases, larger aggregates are obtained, with  $R_h = 7.0$  nm at 50 °C, yet smaller than “pure” T1107 micelles (8.0 nm in hydrodynamic radius).<sup>30</sup>

For both Tetronics (SI, Figures 5 and 6), a bimodal size distribution is obtained, where high aggregates with a hydrodynamic radius of 100 nm are also observed, attributed to clusters of hydrophobic impurities of Tetronics<sup>37,38</sup> and hydrophobic MF aggregates. As temperature increases, impurities are dissolved in micelles and insoluble MF forms soluble mixed micelles, which explains the reduction of aggregates fraction with temperature.

When comparing the SANS patterns as a function of the temperature in the absence or presence of MF, a similar trend to that of TPGS + MF is observed, i.e. a slight reduction in the scattered intensity and a shift of the curves towards the high  $q$  zone occur (Figure 5). The structures of the mixed micelles at 37°C and 50 °C are shown in Figure 5 and SI, Figure 7, respectively, with the corresponding fits to CSS-HS for the different systems poloxamine + MF. The fitted parameters have been gathered in Table 4.

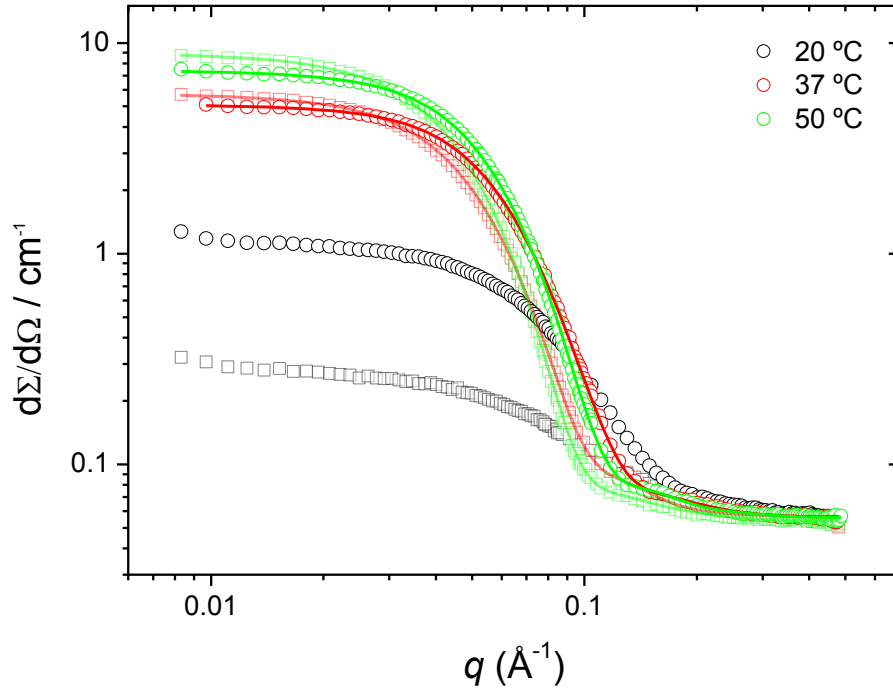


**Figure 5.** SANS curves of 1% T904 ( $\square$ ) and 1% T904 + 0.2% MF ( $\circ$ ) in  $D_2O$  at 20, 37 and 50 °C. Solid lines correspond to the fits to CSS-HS model.

**Table 4.** Structural parameters of Tetronic 904 and T1107 and MF in  $D_2O$  at (A) 37°C and (B) 50 °C deduced from SANS data analysis.  $R_c$  (core radius, Å),  $t$  (shell thickness, Å),  $\phi$  (volume fraction),  $\rho_s$  (shell scattering length density  $\times 10^6 \text{ \AA}^{-2}$ ),  $\rho_c$  (core scattering length density  $\times 10^6 \text{ \AA}^{-2}$ )

| <b>A</b>           | $R_c$ | $t$ | $\phi$ | $\rho_s$ | $\rho_c$ |
|--------------------|-------|-----|--------|----------|----------|
| 1% T904            | 39    | 26  | 0.020  | 6.34     | 0.344    |
| 1% T904 + MF 0.2%  | 30    | 24  | 0.032  | 6.04     | -0.13    |
| 1% T1107           | 31    | 48  | 0.034  | 5.97     | 0.344    |
| 1% T1107 + MF 0.2% | 28    | 46  | 0.049  | 6.03     | -0.79    |

| <b>B</b>          | $R_c$ | $t$ | $\phi$ | $\rho_s$ | $\rho_c$ |
|-------------------|-------|-----|--------|----------|----------|
| 1% T904           | 39    | 25  | 0.021  | 5.79     | 0.344    |
| 1% T904 + MF 0.2% | 34    | 22  | 0.030  | 5.91     | 0.02     |

|                    |    |    |       |      |       |
|--------------------|----|----|-------|------|-------|
| 1% T1107           | 37 | 46 | 0.031 | 5.80 | 0.344 |
| 1% T1107 + MF 0.2% | 32 | 45 | 0.046 | 5.92 | -0.41 |

The same strategy than for the TPGS-MF mixed micelles has been used to analyse the data. In this case,  $sl_{d_{core}}$  of the Tetronic micelles alone was fixed to that of the pure PO ( $\rho_{PO} = 3.44 \times 10^{-7} \text{ \AA}^{-2}$ ), in accordance with previous studies.<sup>28,30</sup> The results for both Tetronics at 37 and 50 °C indicate a reduction in the size of the aggregates when MF is added, in accordance with DLS data, as well as an increase in the volume fraction of micelles compared to Tetronics alone. Those aspects with the fact that lower or negative values of  $sl_{d_{core}}$  are obtained with the addition of MF, point out the formation of the mixed micelles, in which the aromatic moieties of both surfactants are located preferentially in the micelle core, as occur with TPGS. No temperature effect (from 37 °C to 50 °C) is observed either in the size or the volume fraction of those mixed micelles (Table 4).

Once again, the interaction between the MF and the hydrophobic part of the co-surfactant is supported by NMR. The largest changes in the proton spectra occur in the CH<sub>3</sub> signal of the hydrophobic tail of MF (1.07 ppm), which shifts to 1.11 ppm in the presence of the poloxamines, especially with T904 (SI, Figure 8), and reflected in the cross-peak in the 2D-NOESY spectrum between these protons and the CH<sub>3</sub> ones of the POs of the Tetronic (Figure 6). By contrast, methylene protons of the hydrophobic tail of MF (1.23 ppm) and the CH<sub>3</sub> of the hydrophilic head (3.44 ppm) of the MF shift in a lesser extent, while those of the PEO blocks of the poloxamine do not shift (SI, Figure 8). This evidence and the absence of a clear cross-peak between the bulky CH<sub>3</sub> protons of the MF polar head and those of the PPO block of the poloxamine in the 2D-NOESY,

indicate that the MF zwitterion head must not be far from the micelle core, as it happens with TPGS.

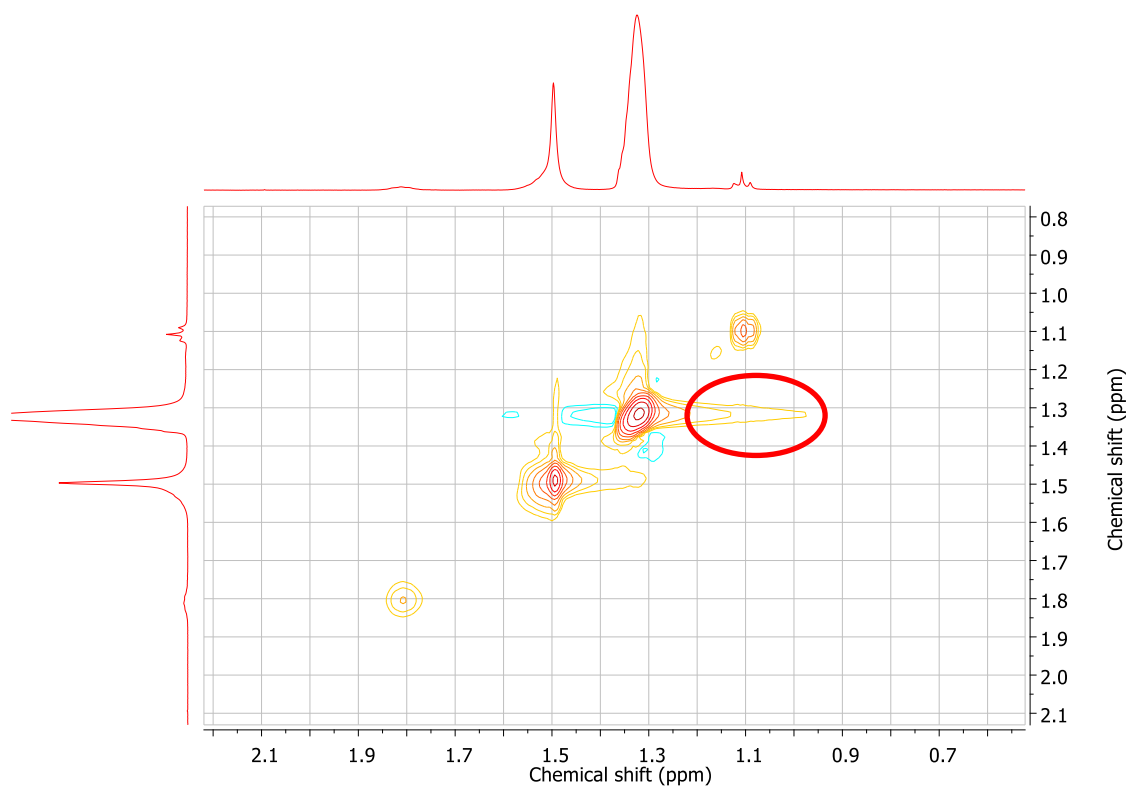


**Figure 6.** Zoomed view of the 2D-NOESY spectrum of 1% T904 + 0.2% MF at 50 °C.

As in the case of the combination of MF with TPGS, the number of unimers of each surfactant in the mixed micelle, can be calculated by solving the system formed by equations (1) and (2). Using the values gathered in Table 4, the water molecules per EO unit of the pure poloxamines at 37 °C are 21.7 and 23.9 for T904 (15 EO groups per arm) and T1107 (60 EO groups per arm), respectively, with 13.8 (T904) and 15.6 (T1107) at 50°C. The results, collected in Table 3, shown how the mixed micelles contain a relatively lower proportion of MF (slightly less in the case of T1107) compared to TPGS. This is a direct consequence of the different structure and sizes of the hydrophobic moieties of TPGS (tocopherol) and the poloxamines (PPO blocks). While TPGS has a hydrophobic part similar to MF, in terms of mass and volume,

Tetronic one is larger and more flexible. Ideally, the more similar the hydrophobic moiety of the co-surfactants, the better compatibility and mixing.<sup>39</sup>

Although the number of Tetronic molecules in mixed micelles increases for T904 and T1107 with temperature, in accordance with Tetronic behaviour, a different MF composition as a function of the Tetronics and temperature is observed. While in T904-MF micelles the number of MF molecules is independent of temperature, T1107-MF micelles require high temperatures to reach the same number of MF molecules (Table 3).

Poloxamine T1107, larger and more hydrophilic than T904 due to the four times longer PEO blocks but nearly the same PPO length, is capable of forming physical gels above 25% and 35°C,<sup>30</sup> which poses the possibility of incorporating the MF in the gels as a potential way of delivery. Figure 7 shows the scattering patterns of 25% T1107 + 0.2% MF, typical of a paracrystal formed by the packing of micelles, with maxima at  $q = 0.55, 0.77$  and  $0.94 \text{ \AA}^{-1}$ .

When comparing, it can be seen how the curves practically match with that of 25 % T1107 in the absence of MF at any temperature (SI, Figure 9). Given the large difference in molar volumes of both surfactants and considering that the molar ratio MF / T1107 is 0.29, it is expected a reduced number of MF molecules per micelle in the dense packing of T1107 micelles, without significant changes in the gel structure. At 37 and 50°C, conditions in which the poloxamine fully forms a gel (SI, Figure 9), the data analysis does not reveal any differences in the absence or presence of MF, when fitting the SANS scattering pattern to a BCC packing of spherical micelles (see SI for details on the mathematical model), typical of this poloxamine.<sup>30</sup> The spheres radius is 34 Å, which practically matches the core of the micelles, and the cell parameter,  $a$ , of the paracrystal is 161 Å. The packing would consist of a BCC network of polydisperse

spheres containing mainly the PPO, with the PEO shells expanding up to a total micelle size of 70 Å according to the calculated dimensions of the paracrystal cell ( $R_{mic}=\sqrt{3/4}a$ ), slightly lower than the size of the micelles at low concentration (Table 4). This indicates the overlapping of the coronas of the micelles in contact to a certain extent, which has also been observed in the larger Tetronic 908 (114 EOs and 21 POs per arm).<sup>31</sup>

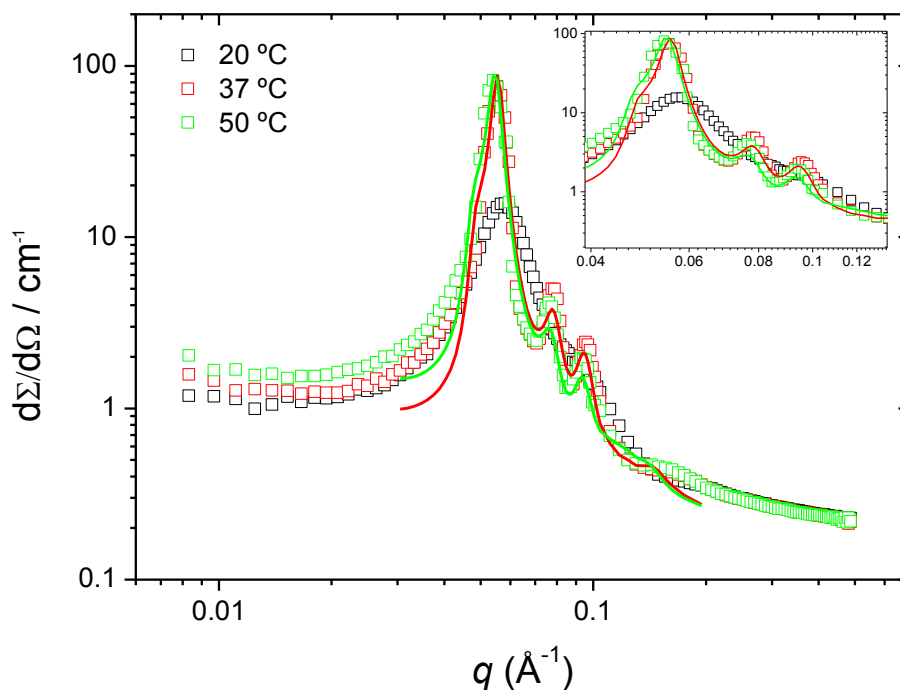


**Figure 7.** SANS curves of 25% T1107 + 0.2% MF in D<sub>2</sub>O at 20, 37 and 50 °C. Solid lines correspond to the fits to a BCC paracrystal.

### 3.3 Biological evaluation of MF-loaded polymeric micelles

After characterizing the structural features of the different MF-polymer systems, we have tested the effect of surfactant-MF systems against *L. major* promastigotes. The results using the MTT assay are summarized in Table 5. It can be seen how the EC<sub>50</sub> of MF alone is  $10.63 \pm 3.65 \mu\text{M}$ , while TPGS, T904 and T1107 alone were not active

against *L. major* promastigotes, with EC<sub>50</sub> values higher than 50 μM. Interestingly, the combination of the three vehicles with MF, makes the drug more active than MF alone against *L. major* promastigotes. In fact, the EC<sub>50</sub> of the formulation T904-MF was significantly lower (\*p<0.05) than that of MF alone which results the most active system in the extracellular form of parasites.

**Table 5.** EC<sub>50</sub> values of studied MF micelles on *L. major* promastigotes 72 hours post-treatment.

| Effect against <i>Leishmania major</i> promastigotes viability |                              |
|--|------------------------------|
| Formulations   | EC <sub>50</sub> (mean ± SD) |
| <b>MF</b>  | 10.63 ± 3.65 μM              |
| <b>TPGS</b>  | >100 μM                      |
| <b>TPGS-MF</b>   | 6.82 ± 0.75 μM               |
| <b>T904</b>  | >50 μM                       |
| <b>T904-MF</b>   | 6.13 ± 1.12 μM (*)           |
| <b>T1107</b>   | >50 μM                       |
| <b>T1107-MF</b>  | 7.01 ± 0.47 μM               |

With the previous results and the fact that T904-MF, T1107-MF and TPGS-MF systems do not exhibit toxicity against murine macrophages (data not shown), we were prompted to assess their activity against *L. major* intracellular amastigotes. *L. major*-infected macrophages were then exposed to different formulations. For each copolymer, surfactant, surfactant-MF(5 μM) and surfactant-MF(10 μM), as well as MF alone (5 μM and 10 μM) samples were studied, where the concentrations 5 and 10 μM correspond to a 1000 and 500 dilution of the stock solution (1% surfactant + 0.2% MF), respectively. The results obtained for T904 and T1107 are compared in Figure 8. While the activity of T904-MF was considerably higher than that of MF alone, especially at low concentrations of the drug, no difference is observed in presence or absence of T1107.

These behaviors can be explained considering previous results and the fact that concentration of surfactants in these studies are highly diluted compare to characterization studies. While T904-MF mixed micelles are completely formed at 37 °C and do not present any temperature effect at 1% T904 + 0.2% MF (Table 3), under biological studies conditions, T904-MF mixed micelles may be formed even at low concentrations (MF 5 µM), enhancing the entrance of MF in infected macrophages. When the concentration of MF and T904 is doubled, the fraction of infected macrophages is reduces compared to T904-MF(5 µM), although MF 10 µm alone presents activity, suggesting and increase in volume fraction of mixed micelles with the concentration without changes in size and composition of the micelles, as observed in Table 3.

Instead, when the longest surfactant is used, micellization behavior of T1107 alone differs from those of T904, requiring more temperature to complete the formation of micelles.<sup>28,30</sup> This aspect explains the behavior of T1107-MF mixed micelles observed in Table 3, where composition of micelles changes from 37 °C to 50 °C. Considering the difficulty of T1107 to micellize at 37 °C added to the fact that lower concentrations are used for biological studies, results shown in Figure 8 suggest that the formation of T1107-MF micelles may not occur under these conditions, where MF micelles may coexist with T1107 unimers, producing the same activity observed for MF micelles.

While this temperature effect explains the Tetronic-MF systems, it cannot explain the results shown for TPGS-MF system, where no different response compare to MF alone is observed (SI, Figure 10). Although more studies are required to understand this behavior, the stability of TPGS micelles with temperature added to the low concentrations used in biological studies and the high aggregation number of TPGS micelles,<sup>27</sup> suggest that TPGS unimers may aggregate each other. Thus, no TPGS is

available to form TPGS-MF micelles and MF micelles are formed, which explains the same behavior observed for MF and TPGS-MF systems.

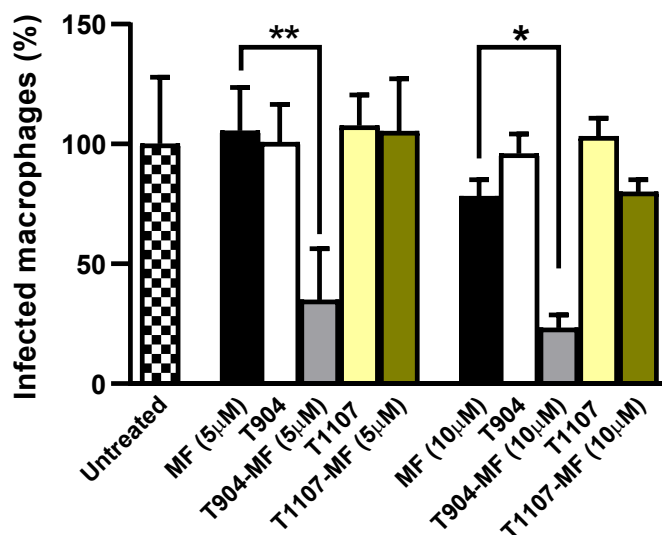


**Figure 8:** Effect of MF, T904, T1107, T904-MF and T1107-MF on *L. major*-infected peritoneal macrophages. Treatments were performed at 5 and 10 μM of MF. Bars represent the percentage of infected macrophages with *L. major* after 72 h of treatment.

#### 4. Conclusions

The combination of MF, a zwitterionic amphiphile used as anti-leishmanial drug, with three polymeric non-ionic surfactants (TPGS, T904 and T1107) has been investigated. SANS studies on MF micelles reveal that the drug self-aggregates into core-shell spheres, without concentration effect from 0.2% to 1%. The micelles are thermally stable, with a slightly decrease in aggregation number as temperature increases.

SANS and NMR experiments show the spherical mixed micelles formed with MF and the three surfactants, where the hydrophobic parts of the drug and the surfactant are in close contact, with a highly hydrated hydrophilic shell mainly formed by the PEG blocks. The aggregation number of MF increases in TPGS-MF mixed micelles compared to MF micelles, observing an enhancement in MF fraction with temperature.

However, different effects are observed depending on the block length when Tetronics are used. While in T904-MF, where the number of MF molecules is independent of temperature, mixed micelles are fully formed at 37 °C, T1107-MF micelles require high temperatures (50 °C) to reach the same number of MF molecules, although, in both cases, lower aggregation numbers are obtained compared to MF micelles. At high concentrations of T1107 (> 20%), the gelation of the system occurs, without influence of MF when low concentrations of the drug are added, revealing a BCC internal structure of the gels.

Biological studies with extracellular promastigotes have been performed for all the systems mentioned, observing a reduction of the EC<sub>50</sub> of the MF in all the formulations compared to MF alone, but being only significant in T904-MF system. Effectiveness of T904-MF is also observed in intracellular amastigotes, allowing a significant higher activity of the MF, especially at low concentrations of the drug (5 µM), while no effect of the surfactant is observed when T1107 and TPGS are used, meaning that spherical mixed micelles under biological conditions are only formed with T904-MF system.

Thus, micelles in a proper formulation, size and shape, can cross layers of the skin and reach the dermis where the burden of Leishmania parasites is normally higher, being the T904-MF a promising formulation for leishmaniasis treatment.

### **Conflict of interests**

The authors declare that have no competing interests.

### **Acknowledgements**

The authors gratefully acknowledge the financial support provided by MINECO (Project MAT2014-59116-C2-2-R), Obra Social La Caixa (LCF/PR/PR13/11080005)

and Fundación Caja Navarra, Gobierno Navarra Salud (12/2017), Fundación Roviralta, Ubesol, Government of Navarre, Laser Ebro, and Fundación Garcilaso de la Vega. JCNS is acknowledged for the access to the KWS-2 diffractometer at the Heinz Maier-Leibnitz Zentrum (MLZ), Garching, Germany. J.P-R. also acknowledges the Asociación de Amigos de la Universidad de Navarra for his doctoral grant.

## References

- (1) Fernández-Rubio, C.; Larrea, E.; Peña-Guerrero, J.; Sesma-Herrero, E.; Gamboa, I.; Berrio, C.; Plano, D.; Amin, S.; Sharma, A. K.; Nguewa, P. A. Leishmanicidal Activity of Isoselenocyanate Derivatives. *Antimicrob. Agents Chemother.* **2019**, *63* (2), 1–12.
- (2) David, C. V.; Craft, N. Cutaneous and Mucocutaneous Leishmaniasis. *Dermatol. Ther.* **2009**, *22* (6), 491–502.
- (3) Fuertes, M. A.; Nguewa, P. A.; Castilla, J.; Alonso, C.; Perez, J. M. Anticancer Compounds as Leishmanicidal Drugs: Challenges in Chemotherapy and Future Perspectives. *Curr. Med. Chem.* **2008**, *15* (5), 433–439.
- (4) Shukla, A. K.; Patra, S.; Dubey, V. K. Evaluation of Selected Antitumor Agents as Subversive Substrate and Potential Inhibitor of Trypanothione Reductase: An Alternative Approach for Chemotherapy of Leishmaniasis. *Mol. Cell. Biochem.* **2011**, *352* (1–2), 261–270.
- (5) Vinson, R. Application for Inclusion of Miltefosine on WHO Model List of Essential Medicines. *Paladin Labs.* **2010**, 21.
- (6) Kapil, S.; Singh, P. K.; Silakari, O. An Update on Small Molecule Strategies Targeting Leishmaniasis. *European Journal of Medicinal Chemistry*. Elsevier Masson SAS September 5, 2018, pp 339–367.
- (7) Nazari-Vanani, R.; Dehdari-Vais, R.; Sharifi, F.; Sattarahmady, N.; Karimian, K.; Motazedian, M. H.; Heli, H. Investigation of Anti-Leishmanial Efficacy of Miltefosine and Ketoconazole Loaded on Nanoniosomes. *Acta Trop.* **2018**, *185*, 69–76.
- (8) Van Bocxlaer, K.; Yardley, V.; Murdan, S.; Croft, S. L. Topical Formulations of Miltefosine for Cutaneous Leishmaniasis in a BALB/c Mouse Model. *J. Pharm.*

- Pharmacol.* **2016**, *68* (7), 862–872.
- (9) Gontijo-Aguiar, M.; Machado-Pereira, A. M.; Fernandes, A. P.; Miranda-Ferreira, L. A. Reductions in Skin and Systemic Parasite Burdens as a Combined Effect of Topical Paromomycin and Oral Miltefosine Treatment of Mice Experimentally Infected with *Leishmania (Leishmania) Amazonensis*. *Antimicrob. Agents Chemother.* **2010**, *54* (11), 4699–4704.
- (10) Soto, J.; Rea, J.; Balderrama, M.; Toledo, J.; Soto, P.; Valda, L.; Berman, J. D. Short Report: Efficacy of Miltefosine for Bolivian Cutaneous Leishmaniasis. *Am. J. Trop. Med. Hyg.* **2008**, *78* (2), 210–211.
- (11) Soto, J.; Arana, B. A.; Toledo, J.; Rizzo, N.; Vega, J. C.; Diaz, A.; Luz, M.; Gutierrez, P.; Arboleda, M.; Berman, J. D.; et al. Miltefosine for New World Cutaneous Leishmaniasis. *Clin. Infect. Dis.* **2004**, *38* (9), 1266–1272.
- (12) Sundar, S.; Jha, T. K.; Thakur, C. P.; Bhattacharya, S. K.; Rai, M. Oral Miltefosine for the Treatment of Indian Visceral Leishmaniasis. *Trans. R. Soc. Trop. Med. Hyg.* **2006**, *100*, 26–33.
- (13) Sundar, S.; Makharia, A.; More, D. K.; Agrawal, G.; Voss, A.; Fischer, C.; Bachmann, P.; Murray, H. W. Short-Course of Oral Miltefosine for Treatment of Visceral Leishmaniasis. *Clin. Infect. Dis.* **2000**, *31* (4), 1110–1113.
- (14) Verma, N. K.; Dey, C. S. Possible Mechanism of Miltefosine-Mediated Death of *Leishmania Donovanii*. *Antimicrob. Agents Chemother.* **2004**, *48* (8), 3010–3015.
- (15) Wasunna, M.; Njenga, S.; Balasegaram, M.; Alexander, N.; Omollo, R.; Edwards, T.; Dorlo, T. P. C.; Musa, B.; Ali, M. H. S.; Elamin, M. y.; et al. Efficacy and Safety of AmBisome in Combination with Sodium Stibogluconate or Miltefosine and Miltefosine Monotherapy for African Visceral Leishmaniasis: Phase II Randomized Trial. *PLoS Negl. Trop. Dis.* **2016**, *10* (9), 1–18.
- (16) Sindermann, H.; Engel, J. Development of Miltefosine as an Oral Treatment for Leishmaniasis. *Trans. R. Soc. Trop. Med. Hyg.* **2006**, *100*, 17–20.
- (17) Calogeropoulou, T.; Angelou, P.; Detsi, A.; Fragiadaki, I.; Scoulica, E. Design and Synthesis of Potent Antileishmanial Cycloalkylidene-Substituted Ether Phospholipid Derivatives. *J. Med. Chem.* **2008**, *51* (4), 897–908.
- (18) Pachioni-Vasconcelos, J. D. A.; Lopes, A. M.; Apolinário, A. C.; Valenzuela-Oses, J. K.; Costa, J. S. R.; Nascimento, L. D. O.; Pessoa, A.; Barbosa, L. R. S.; Rangel-Yagui, C. D. O. Nanostructures for Protein Drug Delivery. *Biomaterials Science*. Royal Society of Chemistry February 1, 2016, pp 205–218.

- (19) Valenzuela-Oses, J. K.; García, M. C.; Feitosa, V. A.; Pachioni-Vasconcelos, J. A.; Gomes-Filho, S. M.; Lourenço, F. R.; Cerize, N. N. P.; Bassères, D. S.; Rangel-Yagui, C. O. Development and Characterization of Miltefosine-Loaded Polymeric Micelles for Cancer Treatment. *Mater. Sci. Eng. C* **2017**, *81* (July), 327–333.
- (20) Feitosa, V. A.; de Almeida, V. C.; Malheiros, B.; de Castro, R. D.; Barbosa, L. R. S.; Cerize, N. N. P.; Rangel-Yagui, C. D. O. Polymeric Micelles of Pluronic F127 Reduce Hemolytic Potential of Amphiphilic Drugs. *Colloids Surfaces B Biointerfaces* **2019**, *180*, 177–185.
- (21) Alexandridis, P.; Hatton, T. A. Poly(ethylene Oxide)-Poly(propylene Oxide)-Poly(ethylene Oxide) Block Copolymer Surfactants in Aqueous Solutions and at Interfaces: Thermodynamics, Structure, Dynamics, and Modeling. *Colloids and Surfaces A: Physicochemical and Engineering Aspects*. March 10, 1995, pp 1–46.
- (22) Su, Y. L.; Wang, J.; Liu, H. Z. FTIR Spectroscopic Investigation of Effects of Temperature and Concentration on PEO-PPO-PEO Block Copolymer Properties in Aqueous Solutions. *Macromolecules* **2002**, *35* (16), 6426–6431.
- (23) Nagarajan, R. Solubilization of Hydrocarbons and Resulting Aggregate Shape Transitions in Aqueous Solutions of Pluronic® (PEO-PPO-PEO) Block Copolymers. *Colloids Surfaces B Biointerfaces* **1999**, *16* (1–4), 55–72.
- (24) Sadoqi, M.; Lau-Cam, C. A.; Wu, S. H. Investigation of the Micellar Properties of the Tocopheryl Polyethylene Glycol Succinate Surfactants TPGS 400 and TPGS 1000 by Steady State Fluorometry. *J. Colloid Interface Sci.* **2009**, *333* (2), 585–589.
- (25) Zhang, Z.; Tan, S.; Feng, S.-S. Vitamin E TPGS as a Molecular Biomaterial for Drug Delivery. *Biomaterials* **2012**, *33* (19), 4889–4906.
- (26) Guo, Y.; Luo, J.; Tan, S.; Oketch, B.; Zhang, Z. The Applications of Vitamin E TPGS in Drug Delivery. *Eur. J. Pharm. Sci.* **2013**, *49* (2), 175–186.
- (27) Puig-Rigall, J.; Grillo, I.; Dreiss, C. A.; González-Gaitano, G. Structural and Spectroscopic Characterization of TPGS Micelles: Disruptive Role of Cyclodextrins and Kinetic Pathways. *Langmuir* **2017**, *33* (19), 4737–4747.
- (28) González-Gaitano, G.; Müller, C.; Radulescu, A.; Dreiss, C. A. Modulating the Self-Assembly of Amphiphilic X-Shaped Block Copolymers with Cyclodextrins: Structure and Mechanisms. *Langmuir* **2015**, *31* (14), 4096–4105.

- (29) González-Gaitano, G.; da Silva, M. A.; Radulescu, A.; Dreiss, C. A. Selective Tuning of the Self-Assembly and Gelation of a Hydrophilic Poloxamine by Cyclodextrins. *Langmuir* **2015**, *31* (20), 5645–5655.
- (30) Serra-Gómez, R.; Dreiss, C. A.; González-Benito, J.; González-Gaitano, G. Structure and Rheology of Poloxamine T1107 and Its Nanocomposite Hydrogels with Cyclodextrin-Modified Barium Titanate Nanoparticles. *Langmuir* **2016**, *32* (25), 6398–6408.
- (31) Puig-Rigall, J.; Obregon-Gomez, I.; Monreal-Pérez, P.; Radulescu, A.; Blanco-Prieto, M. J.; Dreiss, C. A.; González-Gaitano, G. Phase Behaviour, Micellar Structure and Linear Rheology of Tetrablock Copolymer Tetronic 908. *J. Colloid Interface Sci.* **2018**, *524*, 42–51.
- (32) Radulescu, A.; Szekely, N. K.; Appavou, M. S.; Pipich, V.; Kohnke, T.; Ossovyi, V.; Staringer, S.; Schneider, G. J.; Amann, M.; Zhang-Haagen, B.; et al. Studying Soft-Matter and Biological Systems over a Wide Length-Scale from Nanometer and Micrometer Sizes at the Small-Angle Neutron Diffractometer KWS-2. *J. Vis. Exp.* **2016**, No. 118, e54639.
- (33) Macdonald, P. M.; Rydall, J. R.; Kuebler, S. C.; Winnik, F. M. Synthesis and Characterization of a Homologous Series of Zwitterionic Surfactants Based on Phosphocholine. *Langmuir* **1991**, *7* (11), 2602–2606.
- (34) Yaseen, M.; Lu, J. R.; Webster, J. R. P.; Penfold, J. The Structure of Zwitterionic Phosphocholine Surfactant Monolayers. *Langmuir* **2006**, *22* (13), 5825–5832.
- (35) Sanchez-Fernandez, A.; Moody, G. L.; Murfin, L. C.; Arnold, T.; Jackson, A. J.; King, S. M.; Lewis, S. E.; Edler, K. J. Self-Assembly and Surface Behaviour of Pure and Mixed Zwitterionic Amphiphiles in a Deep Eutectic Solvent. *Soft Matter* **2018**, *14* (26), 5525–5536.
- (36) Valero, M.; Castiglione, F.; Mele, A.; da Silva, M. A.; Grillo, I.; González-Gaitano, G.; Dreiss, C. A. Competitive and Synergistic Interactions between Polymer Micelles, Drugs, and Cyclodextrins: The Importance of Drug Solubilization Locus. *Langmuir* **2016**, *32* (49), 13174–13186.
- (37) Polik, W. F.; Burchard, W. Static Light Scattering from Aqueous Poly(ethylene Oxide) Solutions in the Temperature Range 20-90 °C. *Macromolecules* **1983**, *16* (6), 978–982.
- (38) Brown, W. Diffusion of Poly(ethylene Oxide) in Semidilute Aqueous Solution: Dynamic Light Scattering and Gradient Diffusion. *Polymer (Guildf)*. **1985**, *26*

- (11), 1647–1650.
- (39) Moroi, Y. Mixed Micelle Formation. In *Micelles*; Springer US: Boston, MA, 1992; pp 183–194.